PGC-1β controls mitochondrial metabolism to modulate circadian activity, adaptive thermogenesis, and hepatic steatosis

Junichiro Sonoda, Isaac R. Mehl, Ling-Wa Chong, Russell R. Nofsinger, and Ronald M. Evans*

Howard Hughes Medical Institute and Gene Expression Laboratory, The Salk Institute for Biological Studies, La Jolla, CA 92037

Contributed by Ronald M. Evans, December 28, 2006 (sent for review December 21, 2006)

The transcriptional coactivator peroxisome proliferator-activated receptor-γ coactivator 1β (PGC-1β) is believed to control mitochondrial oxidative energy metabolism by activating specific target transcription factors including estrogen-related receptors and nuclear respiratory factor 1, yet its physiological role is not yet clearly understood. To define its function *in vivo*, we generated and characterized mice lacking the functional PGC-1β protein [PGC-1β knockout (KO) mice]. PGC-1β KO mice are viable and fertile and show no overt phenotype under normal laboratory conditions. However, the KO mice displayed an altered expression in a large number of nuclear-encoded genes governing mitochondrial and metabolic functions in multiple tissues including heart, skeletal muscle, brain, brown adipose tissue, and liver. In contrast to PGC-1α KO mice that are reportedly hyperactive, PGC-1β KO mice show greatly decreased activity during the dark cycle. When acutely exposed to cold, the KO mice developed abnormal hypothermia and morbidity. Furthermore, high-fat feeding induced hepatic steatosis and increased serum triglyceride and cholesterol levels in the KO mice. These results suggest that PGC-1β in mouse plays a nonredundant role in controlling mitochondrial oxidative energy metabolism.

knockout mice | oxidative metabolism | energy metabolism | lipogenesis

Mitochondria serve as the cellular powerhouse that generates ATP or heat by using substrates derived from fat and sugar. Highlighting the importance of this process is the fact that mitochondrial dysfunction is implicated in aging and the development of a plethora of clinical symptoms. For example, mutations in mtDNA or nuclear DNA (nDNA) that affect mitochondrial oxidative metabolism contribute to Alzheimer's and Parkinson's diseases, various forms of cancer, and disorders of the respiratory, cardiac, gastrointestinal, endocrinal, ophthalmological, and nervous systems (1). Defects in mitochondrial fatty acid β-oxidation (FAO) or the electron transport chain also lead to hepatic steatosis (fatty liver) in humans and mice (2). In addition, insulin resistance is associated with a coordinate reduction in nDNA-encoded mitochondrial gene expression and mitochondrial ATP synthesis and an increase in skeletal muscle lipid content (3). In mice, a defect in mitochondrial FAO (4) or uncoupling protein-1 (UCP-1) (5) causes a defect in brown adipocyte-mediated thermogenesis.

Nuclear receptors are pleiotropic regulators of glycolytic and oxidative metabolism (6). Studies over the last decade have revealed that mitochondrial activity is transcriptionally controlled, in part, by the nuclear receptors and the peroxisome proliferator-activated receptor-γ coactivator 1 (PGC-1)-related protein family (7, 8). PGC-1α was the first and is by far the most characterized member of the PGC-1 family. In addition to broadly activating nuclear receptors, it directly interacts with other DNA-binding transcription factors, inducing mRNA transcription through two conserved domains, the N-terminal activation domain (9) and the C-terminal RNA-recognition domain (10). Notably, PGC-1α potently induces the expression of genes implicated in energy homeostasis in almost every cell type through known mitochondrial regulators such as the estrogen-related receptors (ERRs), peroxisome proliferator-activated receptor δ, or nuclear respiratory factor 1 (7, 8, 11, 12). Overexpression of PGC-1α in skeletal muscle cells results in an increased energy expenditure, mitochondrial biogenesis (13, 14), and induction of oxidative slow-twitch fibers (15), whereas loss of PGC-1α results in reduced muscle performance, thermogenic defects during acute cold exposure, cardiac defects, and other metabolic and behavioral defects (16, 17).

PGC-1β was identified by its high sequence similarity with PGC-1α (18, 19), and its tissue distribution pattern is also very similar to PGC-1α with high expression detected in oxidative tissues such as brown adipose tissue (BAT), heart, and slow-twitch soleus muscle (19–21). PGC-1β activates all three subtypes of ERRs and nuclear respiratory factor 1, but not many other PGC-1α targets (22, 23). Indeed, overexpression of PGC-1β leads to induction of a small subset of PGC-1α target genes, most of which are implicated in mitochondrial oxidative metabolism and other related functions (22). Consistent with this finding, PGC-1β overexpression results in an increased mitochondrial respiration in cultured cells (14) and higher energy expenditure and resistance to obesity in transgenic mice (23). Functional redundancy between PGC-1α and PGC-1β was suggested by a recent study (24) using immortal brown adipocyte lines that has shown that knocking PGC-1β by specific siRNA reduces expression of ERRα or nDNA-encoded mitochondrial genes only when the cells also carry a genetic deletion of PGC-1α gene. In addition to regulation of mitochondrial energy metabolism, PGC-1β has been suggested to control hepatic lipogenesis and very low density lipoprotein secretion through regulation of sterol regulatory element-binding proteins (SREBPs), liver X receptors, and FOXA2 in the liver (25, 26). These transcription factors appear to be selective PGC-1β targets and are not activated by PGC-1α.

Although the studies described above implicate PGC-1β as a key regulator of oxidative energy metabolism and hepatic lipid metabolism, the majority of knowledge has come from overexpression studies or siRNA-mediated transient gene knockdown. Here, we report the generation and characterization of mice with targeted deletion of the PGC-1β gene. PGC-1β knockout (KO) mice displayed altered expression of many genes required for mitochondrial energy metabolism, showed severe sensitivity to acute cold exposure, and developed hepatic steatosis upon

Author contributions: J.S. and R.M.E. designed research; J.S. and L.-W.C. performed research; J.S. and R.R.N. contributed new reagents/analytic tools; J.S. and I.R.M. analyzed data; and J.S. and R.M.E. wrote the paper.

The authors declare no conflict of interest.

Abbreviations: BAT, brown adipose tissue; ERR, estrogen-related receptor; FAO, fatty acid β-oxidation; FFA, free fatty acid; GTT, glucose tolerance test; HFD, high-fat diet; ITT, insulin tolerance test; KO, knockout; nDNA, nuclear DNA; PGC-1, peroxisome proliferator-activated receptor-γ coactivator 1; Q-PCR, quantitative PCR; SREBP, sterol regulatory element-binding protein; TG, triglyceride; UCP, uncoupling protein; WAT, white adipose tissue.

*To whom correspondence should be addressed. E-mail: evans@salk.edu.

© 2007 by The National Academy of Sciences of the USA

PHYSIOLOGY

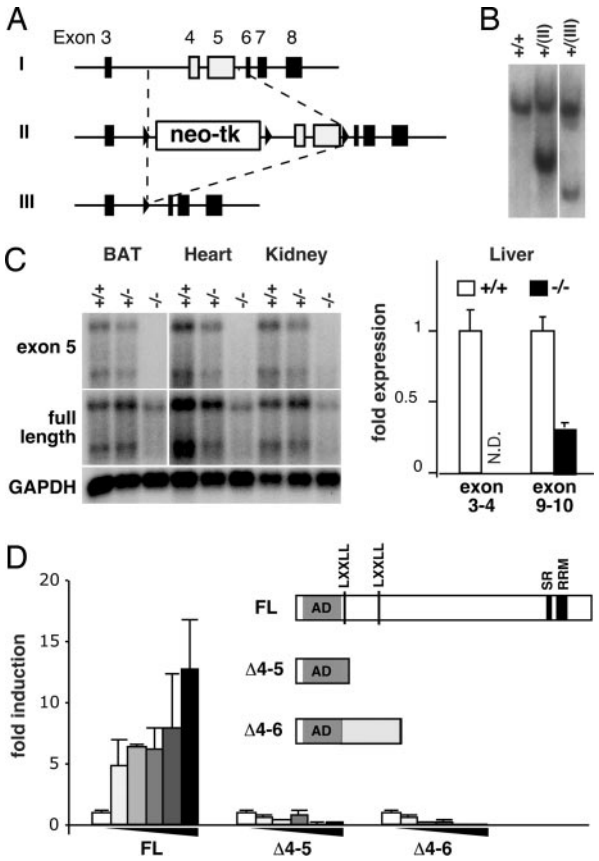

Fig. 1. Strategy and analysis of PGC-1β gene targeting. (*A*) PGC-1β targeting strategy. A targeting construct was introduced into the genomic PGC-1β locus (*I*), yielding homologous recombination loci (*II*). Cre recombination in ES cells further yielded the KO loci, which lacks exons 4 and 5 (*III*). (*B*) Southern blot analysis of targeted ES cell lines. (*C*) Northern blot (*Left*) and Q-PCR (*Right*) analyses of PGC-1β mRNA expression. (*Left*) cDNA encoding a part of exon 5 (*Top*) or the entire PGC-1β (*Middle*) was used to probe total RNA isolated from BAT, heart, and kidney. (*Bottom*) GAPDH was used as a loading control. For heart and kidney, x-ray film was exposed longer than for BAT. (*Right*) Primer pairs spanning exons 3–4 or 10–11 were used to quantify PGC-1β mRNA levels in livers. N.D., not detected. (*D*) Predicted primary structure of WT and mutant PGC-1β proteins and their activity in a transient transfection assay for activation of ERRα is shown. The activation domain (AD), the serine/arginine-rich domain (SR), and the RNA-recognition motif (RRM) conserved among all three PGC-1 family members, and the LXXLL nuclear receptor interaction motifs conserved between mouse and human PGC-1β are indicated. The murine PGC-1β harbors an additional nonconserved LXXLL sequence within the AD. The graph shows that WT but not the PGC-1β mutants induces transcription of a UAS-driven luciferase reporter gene in HEK293 cells through ERRα ligand-binding domain fused to GAL4 DNA binding domain (GAL-ERRαLBD) in a dose-dependent manner. The results represent the average of triplicate experiments for the luciferase activity normalized by β-gal activity.

feeding of a high-fat diet (HFD). These results demonstrate a nonredundant role for PGC-1β in coordinately regulating a network of genes important for mitochondrial function.

Results

To understand the role of PGC-1β *in vivo*, a mouse line harboring deletion of exons 4 and 5 of the PGC1-β gene was created by using homologous recombination in ES cells followed by CRE-mediated recombination as outlined in Fig. 1*A*. Both Southern blot and PCR analyses confirmed the correct targeting event in the ES cells and the mouse line obtained (Fig. 1*B* and data not shown). Heterozygous crossings gave rise to homozygous mutant offspring mice (PGC-1β KO) at a lower than Mendelian frequency at weaning (male WT/heterozygote/KO = 30%:53%:17%; n = 412). However, the surviving PGC-1β KO mice appeared to develop normally without overt developmental, fertility, or growth defects (data not shown). Northern blot and quantitative PCR (Q-PCR) mRNA analyses indicated that the mutant mRNA lacks both targeted exons 4 and 5 as expected, but is expressed in various tissues at lower, but detectable, levels (Fig. 1*C*). To determine the nature of the mutant mRNA expressed, we sequenced eight cDNA clones obtained from BAT of PGC-1β KO mice and found that seven clones had deletion of exons 4 and 5 as predicted, and one clone had deletion of exons 4–6, both resulting in a frameshift mutation after amino acid 176 (Fig. 1*D*). The mutant proteins are predicted to contain the entire N-terminal presumptive activation domain, but lack the two conserved nuclear receptor binding LXXLL signature motifs, centrally located putative binding regions for SREBPs and FOXA2, and the conserved C-terminal RRM motif essential for the activity of PGC-1α (Fig. 1*D*). Neither of the PGC-1β mutants were able to activate an ERRα ligand binding domain fused to GAL4 DNA binding domain in a cell-based reporter assay (Fig. 1*D*). Collectively, these results established that the PGC-1β KO mice lack functional PGC-1β protein.

Although transgenic overexpression of PGC-1β in skeletal muscle has been reported to result in increased fat oxidation and energy expenditure (23), the loss of PGC-1β in mice did not affect O_2 consumption, CO_2 production, or respiratory exchange ratio (Fig. 2*A* and data not shown). The KO mice consumed normal amounts of chow and maintained normal body weights up to at least 6 months of age (data not shown). In contrast to PGC-1α KO mice that have been reported to be hyperactive (16), PGC-1β KO mice showed greatly decreased activity during the dark cycle (Fig. 2*A*). This phenotype is unlikely caused by reduced muscle or cardiac performance, because KO mice displayed comparable running endurances when subjected to involuntary exercise on a treadmill (Fig. 2*B*). Paradoxically, serum analysis indicated that PGC-1β KO mice have reduced serum triglyceride (TG) and free fatty acid (FFA) levels, despite our expectation that loss of PGC-1β and the resulting FAO defects would increase serum TG and FFA levels (Fig. 2*C*). Gene expression analysis revealed that the expression of PGC-1α and a target transcription factor ERRγ is increased in heart (ventricle), slow-twitch oxidative soleus muscle, and brain (cerebellum) of KO mice, which may explain the lowered serum TG and FFA levels (Fig. 2*D*). However, we also found that the expression of a number of mitochondrial genes is reduced in KO mice, indicating a nonredundant role for PGC-1β in these tissues (Fig. 2*D*).

In rodents, PGC-1β is constitutively expressed at high levels in BAT (19–21). As the main function of BAT is UCP-1-mediated nonshivering thermogenesis during cold exposure (4, 5, 27), we tested whether PGC-1β KO mice retained a normal adaptive thermogenic function. When acutely exposed to 4°C from thermoneutrality, PGC-1β KO mice show dramatic hypothermia and morbidity, whereas WT mice tolerate the same procedure (Fig. 3*A*). Three hours after cold exposure, the difference in the core body temperature between WT and KO reached statistical significance ($P < 0.003$). Five hours after cold exposure, the core temperature was between 34.4°C and 36.5°C for WT mice, whereas it was 20.0°C and 31.7°C for KO mice. Although overexpression of PGC-1β has been reported to induce mitochondrial biogenesis, no changes in mtDNA-to-nDNA copy number ratio in BAT or two other oxidative tissues, soleus muscle and heart, were detected by Q-PCR (Fig. 3*B*). The cold sensitive phenotype of the PGC-1β KO mice is reminiscent of mice lacking Ucp-1 (5), PGC-1α (16, 17), or fatty acid acyl-CoA dehydrogenases (4). Mice lacking deiodinase 2 have also been reported to have a subtle cold sensitivity (28). Q-PCR analyses revealed no defects in temperature-dependent regulation of Ucp-1 expression and an increased expression of PGC-1 α and

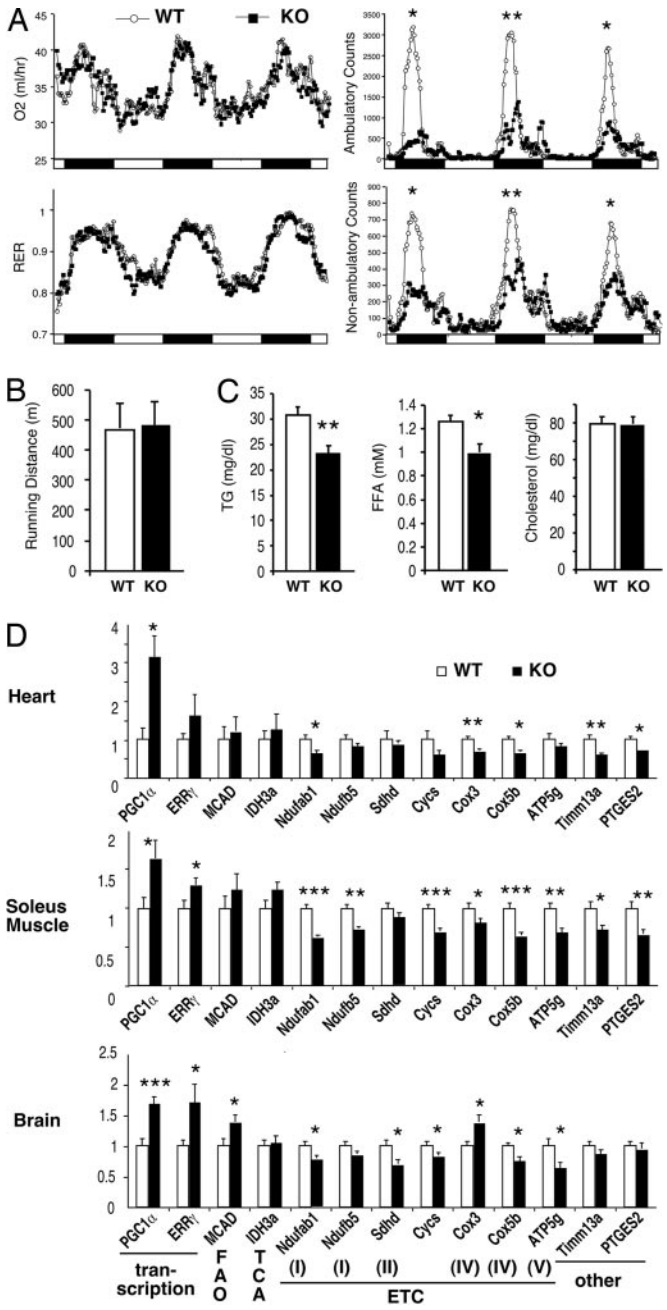

Fig. 2. Basal metabolic analysis of PGC-1β KO mice. (*A*) O_2 consumption, respiratory exchange ratio (RER), and activity of 7- to 9-week-old weight-matched WT (○) and KO (■) mice as measured by metabolic chambers. Light cycle (open bars) and dark cycle (filled bars) are indicated at the bottom. The data shown are the average of four mice for each genotype and represent results from multiple experiments using 12 mice for each group. *, $P < 0.05$; **, $P < 0.005$ at the peaks. (*B*) Running distance on an involuntary treadmill. (*C*) Serum lipid analysis of 8- to 9-week-old weight-matched mice. *, $P < 0.01$; **, $P < 0.002$. $n = 12$. (*D*) Q-PCR mRNA expression analysis in heart (ventricles; *Top*), skeletal muscle (soleus; *Middle*), and brain (cerebellum; *Bottom*). $n = 6–8$. *, $P < 0.05$; **, $P < 0.01$; ***, $P < 0.0005$. The gene functions are indicated at the bottom.

deiodinase 2 in PGC-1β KO BAT tissue after 5 h of cold exposure. However, the expression of nDNA- and mtDNA-encoded genes functioning in mitochondrial FAO (VLCAD) and subunits of the electron transport chain (NADH dehydrogenase ubiquinone flavoproteins, cytochrome *c*, cytochrome *c* oxidase, etc.) are significantly reduced in BAT in the KO mice before the cold exposure (Fig. 3*C*). Reduction in BAT mitochondrial gene expression was confirmed by genomewide expression analysis using Affymetrix (Santa Clara, CA) oligo DNA microarrays (Table 1). These results suggest that PGC-1β is essential for sustaining a high oxidative metabolism to generate enough heat to survive acute cold exposure.

Another condition in which organisms need to maintain a high level of oxidative metabolim is when fat intake is in excess of the caloric requirement. To test the response of PGC-1β KO mice to a Western-style diet, KO and control WT mice were fed a HFD containing 35% saturated fat. On the HFD, PGC-1β KO gained weight at a rate similar to WT control mice (Fig. 4*A*), and after 7–8 weeks on the HFD, showed a normal response to glucose tolerance test (GTT) and insulin tolerance test (ITT) (Fig. 4*B*). However, after 12 weeks on the HFD, the KO mice showed an increased liver-to-body-weight ratio, whereas the ratio of epididymal white adipose tissue (WAT) to body weight was not significantly changed (Fig. 4*C*). Hepatic lipid analysis showed a dramatic 75% increase in TG levels in the HFD-fed KO liver compared with HFD-fed WT liver (Fig. 4*D*). Consistent with these results, hematoxylin and eosin staining revealed the presence of large lipid droplets in livers of HFD-fed KO mice. Serum TG and FFA levels were also elevated in HFD-fed KO mice (Fig. 4*E*), despite the reduced serum TG levels in chow-fed PGC-1β KO (Figs. 2*C* and 4*F*). Furthermore, HFD-fed KO mice showed increased serum total cholesterol levels.

To gain insights into the mechanism by which the loss of PGC-1β results in lipid accumulation in the HFD-fed liver and elevated serum TG and cholesterol, we examined the expression of genes implicated in lipid clearance and synthesis. In WAT, we detected elevated expression of PGC-1α and reduced expression of very few mitochondrial genes including *CytC*, *Cox1*, and *Cox2* (Fig. 4*G*). Conversely, the expression of a large number of genes required for mitochondrial functions was altered in KO livers (Fig. 4*H*). Remarkably, expression of lipogenic genes known to be regulated by the SREBP transcription factors (29) were coordinately increased in the HFD-fed liver despite the fact that the KO livers accumulate more lipids under HFD-fed conditions (Fig. 4*H*). Genomewide expression analysis using Affymetrix oligo DNA microarrays indicated that mitochondrial function and cholesterol biosynthesis are indeed the major Gene Ontology pathways dysregulated in the liver of HFD-fed PGC-1β KO mice (Table 2). Thus, PGC-1β is required for hepatic lipid breakdown and suppression of hepatic lipid synthesis in response to increased dietary fat intake.

Discussion

Our results demonstrated that PGC-1β is an essential factor in mice for normal energy metabolism. Although expression of PGC-1α is elevated in the absence of PGC-β in all of the tissues that we examined, this compensatory increase in PGC-1α is not sufficient to prevent acute cold sensitivity, HFD-induced hepatic steatosis, and other metabolic and behavioral defects in PGC-1β KO mice. Acute cold sensitivity and/or hepatic steatosis have been observed for other mouse models with defects in mitochondrial oxidative metabolism and energy uncoupling (4, 5, 16, 17, 30). Indeed, coordinate reduction in nDNA- and mtDNA-encoded mitochondrial genes was observed in multiple tissues in PGC-1β KO mice. Thus, while conceivably overlapping, the function of PGC-1α and PGC-1β in the regulation of mitochondrial function is nonredundant.

While this article was in preparation, Vianna *et al.* (31) and Lelliott *et al.* (32) reported independent mouse lines in which the PGC-1β gene was targeted. Lelliott *et al.* used a targeting strategy similar to ours, deleting exons 4 and 5, thus most likely resulting in expression of nonfunctional proteins (Fig. 1). In Vianna *et al.*'s line, a deletion of exons 3 and 4 results in

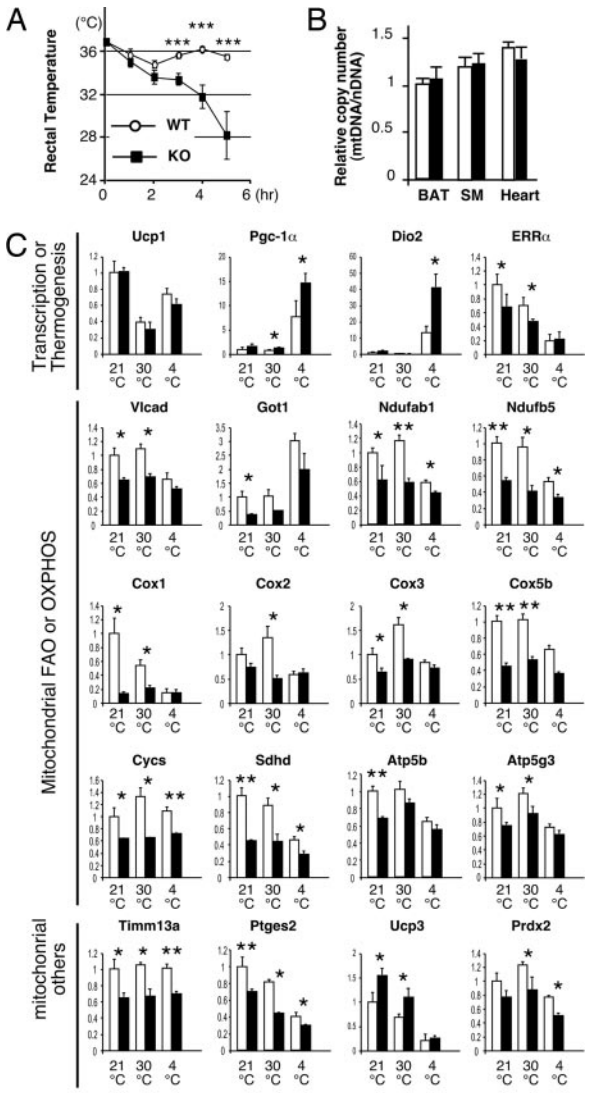

Fig. 3. PGC-1β KO mice are cold-sensitive. (*A*) Rectal temperature of 6- to 9-week-old weight-matched WT (○) and KO (■) mice during exposure to 4°C. Before the cold exposure, mice were acclimated to thermoneutrality (30°C). $n = 7$; ***, $P < 0.005$. (*B*) Q-PCR analysis of mtDNA level normalized by the nDNA level. Total DNA isolated from BAT, soleus muscle (SM), and heart was subjected to Q-PCR analysis. No difference was observed between 9- and 14-week-old WT (open bars) and KO (filled bars) mice. $n = 13$ (WT) and 7 (KO). (*C*) Q-PCR mRNA expression analysis in BAT. Total RNA was isolated from WT (open bars) and KO (filled bars) mice maintained at 21°C or 30°C or exposed to 4°C for 5 h after acclimation at 30°C. $n = 4$–5. *, $P < 0.05$; **, $P < 0.01$.

hypomorphic mutant protein lacking an internal 110-aa stretch that retains a substantial activity toward ERRα, the host cell factor, and SREBP-1c in transient transfection assays. Although there are some differences in targeting strategies, genetic backgrounds, and laboratory conditions, which may have resulted in the differences seen between the three PGC-1β KO strains, expression of nDNA-encoded mitochondrial genes are dysregulated in all three lines, confirming the early proposal that PGC-1β regulates mitochondrial function. Studies of all three lines also agree that PGC-β KO mice accumulate TG in the liver under certain conditions. Modestly increased hepatic TG levels in chow-fed KO mice was observed in both our line (Fig. 4*D*) and Vianna *et al.*'s line (31). This phenotype is more pronounced when the KO mice are fed a diet containing hydrogenated

Table 1. Gene Ontology terms that were down-regulated ($P < 1 \times 10^{-11}$) in KO BAT at 21°C compared with WT BAT

GO terms	No. of features
Cytoplasm	47
Mitochondrion	40
Generation of precursor metabolites and energy	20
Inner membrane	15
Oxidoreductase activity	18
Monovalent inorganic cation transporter activity	11
Primary active transporter activity	7
Sodium ion transporter activity	7
NADH dehydrogenase (ubiquinone) activity	7
Membrane-bound organelle	49
Intracellular membrane-bound organelle	49
Mitochondrial membrane	16
Oxidoreductase activity on NADH or NADPH	7
Mitochondrial inner membrane	15
Electron transport	15

No Gene Ontology (GO) terms were significantly up-regulated ($P < 1 \times 10^{-10}$). A similar result was obtained with BAT RNA isolated from mice after 5 h of acute cold exposure (data not shown).

vegetable oil (saturated transfat) for 24 h (32) or a diet containing saturated animal fat for 12 weeks (Fig. 4 *D* and *E*), indicating the inability of PGC-1β KO mice to efficiently clear out excess dietary lipid. Although the mechanisms causing the lipid accumulation in these two cases are not clear, our gene expression analysis suggests that dysregulation of the lipogenic program due to uncontrolled SREBP target gene expression may be involved (Fig. 4*H*).

Our analysis demonstrated that the PGC-1β KO mice cannot tolerate acute cold exposure, although the work by Lelliott *et al.* (32) has shown that PGC-1β KO mice could gradually acclimate to 4°C. These two observations are seemingly paradoxical, but in fact also hold true for UCP-1 KO mice that completely lack the thermogenic response to β-adrenargic stimuli in brown adipocytes. In the case of UCP-1 KO mice, it is believed that UCP-1-independent thermogenesis in both skeletal muscle and WAT is acquired during cold acclimation to compensate for the loss of UCP-1 (33, 34). Whether this is also the case for PGC-1β KO mice remains a question for future investigation. Another phenotype unique to our strain is significantly lowered physical activity during the dark cycle (Fig. 2*A*). Although we do not currently understand the basis for such inactivity, we could speculate that PGC-1β, like its close homologue PGC-1α (16, 17, 35), may be required for the proper function of the central nervous system controlling the circadian motor activity. PGC-1β is expressed at high levels in the brain, particularly in the cerebellum, which controls sensory perception and motor output (21). Furthermore, PGC-1α and various mitochondrial genes are

Table 2. Gene Ontology (GO) terms that were differentially expressed ($P <$ 2E-09) between HFD-WT and HFD-KO livers

GO terms	No. of features	*P* value
Oxidoreductase activity*	34	0
Sterol biosynthesis†	10	0
Cholesterol biosynthesis†	10	0
Cytoplasm*†	84	0
Generation of precursor metabolites and energy*	26	1.0E-10
Mitochondrion*	33	8E-10
Electron transport*	20	1.7E-09

*, Down-regulated in KO livers; †, up-regulation in KO liver.

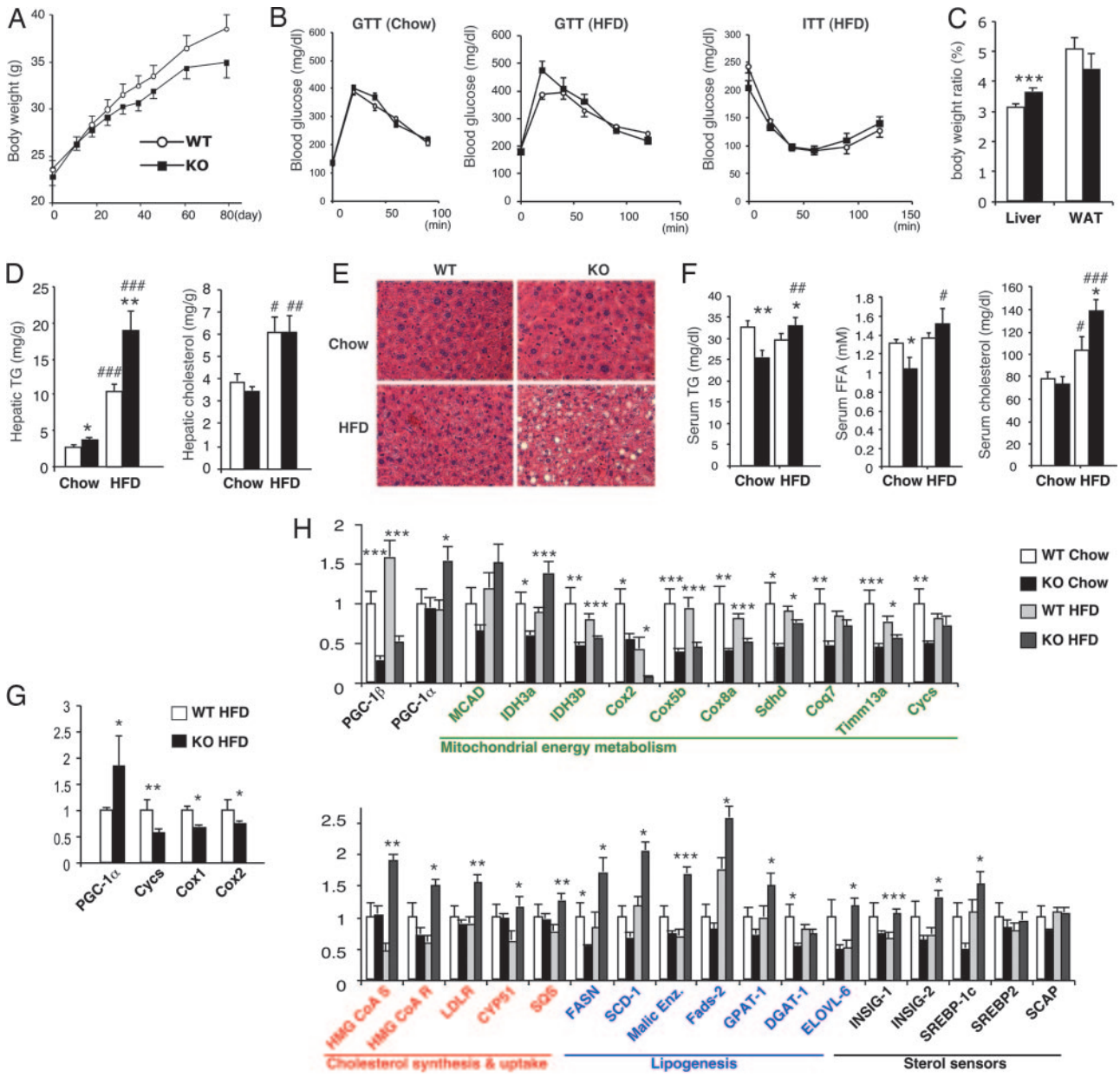

Fig. 4. HFD-induced hepatic steatosis in PGC-1β KO mice. (*A*) Weight gain of WT (○) and KO (■) mice on a HFD. The initial ages of mice were 8–11 weeks old ($n = 12$). Some PGC-1β KO mice started losing weight after 7 weeks on a HFD (data not shown). Statistical significance was not reached. (*B*) GTT or ITT were performed with weight-matched chow-fed 15-week-old mice (*Left*), 15-week-old mice fed HFD for 8 weeks (*Center*), or 14-week-old mice fed HFD for 7 weeks (*Right*). WT (○) and KO (■) mice were fasted overnight for GTT or 4 h for ITT, and then 1.5 g/kg glucose (*Left*), 1g/kg glucose (*Center*), or 1 unit/kg human insulin (*Right*) was injected i.p. at $T = 0$. $n = 10$. (*C*) Liver and epididymal WAT weights of WT (open bar) and KO (filled bar) mice normalized by total body weight after 12 weeks on HFD. $n = 12$. (*D*) Hepatic TG and cholesterol of WT (open bars) and KO (filled bars) mice. Twenty- to 23-week-old HFD-fed mice and 23- to 24-week-old chow-fed mice were used. $n = 7$. The mean body weights were 32.9 ± 0.43 g (WT-Chow), 32.3 ± 0.47 g (KO-Chow), 36.6 ± 1.49 (WT-HFD), and 36.5 ± 1.17 g (KO-HFD). *, $P < 0.05$; **, $P < 0.01$ versus WT; #, $P < 0.05$; ##, $P < 0.005$, ###, $P < 0.0001$ versus chow-fed. (*E*) Representative H&E staining of livers. Note the accumulation of large lipid droplets in HFD-fed KO livers. (*F*) Serum analysis of WT (open bars) and KO (filled bars) mice used in *D*. $n = 7$. *, $P < 0.05$; **, $P < 0.01$ versus WT. #, $P < 0.05$; ##, $P < 0.01$; ###, $P < 0.0001$ versus chow-fed. (*G*) Q-PCR mRNA expression analysis in WAT of HFD-fed mice used in *D*. $n = 7$. *, $P < 0.05$; **, $P < 0.01$. (*H*) Q-PCR mRNA expression analysis in livers of chow-fed and HFD-fed WT and KO mice used in *D*. Black, metabolic regulation; green, mitochondrial function; red, cholesterol synthesis and uptake; and blue: lipogenesis. $n = 7$. *, $P < 0.05$; **, $P < 0.01$; ***, $P < 0.005$.

dysregulated in the cerebellum of PGC-1β KO mice (Fig. 2*D*). Future dissection of PCG-1β function in the brain may shed new light on the role of this protein in the etiology and treatment of neurodegenerative disorders.

In summary, our analysis established a role for PGC-1β to regulate the metabolic gene network required for the proper mitochondrial function in mice. This regulation becomes particularly important under metabolic stress such as acute cold exposure or HFD feeding, underscoring the requirement for optimal mitochondrial activity in these conditions. As the loss of PGC-1β appears partially compensated by an elevated expression of PGC-1α, generation of mice lacking both PGC-1α and PGC-1β is of particular interest in elucidating the full picture of the transcriptional regulation of mitochondrial function by the PGC-1 family.

Methods

Generation of PGC-1β KO Mice. The targeting vector was constructed by inserting three pieces of BAC genomic DNA clone encoding the murine PGC-1β gene locus (Invitrogen, Carlsbad, CA) into pFlox (a gift from Jamey D. Marth, University of California at San Diego, La Jolla, CA) and electroporated into murine SV129 ES cell line. G418-resistant clones were selected by PCR and Southern blot for the appropriate homologous recombination event at both 5′ and 3′ ends. The selected clones were further electroporated with the CMV-NLS-CRE plasmid, and 1-(2′-deoxy-2′-fluoro-β-D-arabinofuranosyl)-5-iodouracil-resistant clones were selected by PCR and Southern blot for the appropriate recombination event, which eliminated the floxed insertion. The resulting ES clones were injected into C56BL/6J blastocysts. Chimeras were mated to C57BL/6J, and germ-line transmission was confirmed by PCR and Southern blot of tail DNA.

Animal Studies. All of the experiments were performed with age-matched male mice from heterozygote crosses that were back-crossed four to six times with the aid of Genome Scan (Jackson Laboratory, Bar Harbor, ME), which estimated that ≈94–99% of the genome in the mice used for the study is derived from C57BL/6J. Mice were maintained in a pathogen-free animal facility at 21°C under standard 12-h light/12-h dark cycle with access to chow [either a standard rodent chow (Labdiet 5001, 4.5% fat, 4.00 kcal/g) or a high-fat, high-carbohydrate diet (Bio-Serv F3282, 35.5% fat, 5.45 kcal/g)] and given water ad libitum. Indirect calorimetric studies were conducted in a Comprehensive Lab Animal Monitoring System (eight-chamber system, Columbus Instruments, Columbus, OH). Total cholesterol, TG, and FFA were determined by using enzymatic reactions (Thermo DMA; FFA, Roche, Minneapolis, MN). For hepatic lipid analysis, the lipid was extracted according to the Folch method and resuspended in PBS containing 5% Triton X-100. For the acute cold exposure study, rectal temperature was measured with a clinical monitoring thermometer (model TH-5; Physitemp Thermalert, Clifton, NJ) every 60 min until any of the mice showed hypothermia (body temperature <25°C). For GTT and ITT, glucose level was measured with a One Touch Ultra glucometer (LifeScan, Milpitas, CA). Human insulin (Humilin; Eli Lily, Indianapolis, IN) was used for ITT. Statistics were performed by Student's *t* test. Values were presented as means ± SEMs. All protocols for mouse experiments were approved by the Institutional Animal Care and Use Committee of The Salk Institute.

Gene Expression Analysis. SYBR green (Invitrogen) was used for Q-PCR mRNA expression analysis with 36B4 as a control. For DNA microarray analysis, labeled poly(A) RNA ($n = 3$) were hybridized to Affymetrix mouse genome 430 2.0 arrays. Background correction, normalization, and expression values were obtained by using RMA. Significant difference was defined by fold change >1.5 and $P < 0.005$. Subsequently, the VAMPIRE microarray analysis suite (http://biome.sdsc.edu:8090/vampire) was used for GO analysis. For Q-PCR DNA analysis, total DNA digested with NotI was used. Primer sequences will be provided on request.

Note Added in Proof: It has recently been reported that mice lacking estrogen-related receptor α display thermogenic defects similar to PGC-1β KO mice described here (36).

We thank Lita Ong and Sally Ganley for administrative assistance; Ruth Yu and Liming Pei for critical reading of the manuscript; Mike Nelson, Henry Juguilon, Yu-Hua Zou, The Salk Microarray Facility, and University of California at San Diego histology resources, for technical assistance; and Natasha Kralli and Pep Villena for suggestions. R.M.E. is an Investigator of the Howard Hughes Medical Institute and March of Dimes Chair in Molecular and Developmental Biology. This work was supported by Damon Runyon Cancer Research Foundation Fellowship DRG 1711-02 (to J.S.), the American Heart Association (J.S.), National Institutes of Health/National Institute of Diabetes and Digestive and Kidney Diseases Nuclear Receptor Signaling Atlas Program Grant U19DK62434-01 (to R.M.E.), Environmental Protection Agency Superfund Program Grant P42 ES10337 (to R.M.E.), National Institutes of Health Grants 5R37 DK057978 and 5R01 HD027183 (to R.M.E.), and the Howard Hughes Medical Institute (R.M.E.).

1. Wallace DC (1999) *Science* 283:1482–1488.
2. Pessayre D, Berson A, Fromenty B, Mansouri A (2001) *Semin Liver Dis* 21:57–69.
3. Petersen KF, Shulman GI (2006) *Am J Med* 119:S10–S16.
4. Guerra C, Koza RA, Walsh K, Kurtz DM, Wood PA, Kozak LP (1998) *J Clin Invest* 102:1724–1731.
5. Enerback S, Jacobsson A, Simpson EM, Guerra C, Yamashita H, Harper ME, Kozak LP (1997) *Nature* 387:90–94.
6. Mangelsdorf DJ, Thummel C, Beato M, Herrlich P, Schutz G, Umesono K, Blumberg B, Kastner P, Mark M, Chambon P, *et al.* (1995) *Cell* 83:835–839.
7. Lin J, Handschin C, Spiegelman BM (2005) *Cell Metab* 1:361–370.
8. Finck BN, Kelly DP (2006) *J Clin Invest* 116:615–622.
9. Puigserver P, Adelmant G, Wu Z, Fan M, Xu J, O'Malley B, Spiegelman BM (1999) *Science* 286:1368–1371.
10. Monsalve M, Wu Z, Adelmant G, Puigserver P, Fan M, Spiegelman BM (2000) *Mol Cell* 6:307–316.
11. Wang YX, Lee CH, Tiep S, Yu RT, Ham J, Kang H, Evans RM (2003) *Cell* 113:159–170.
12. Giguere V (2002) *Trends Endocrinol Metab* 13:220–225.
13. Wu Z, Puigserver P, Andersson U, Zhang C, Adelmant G, Mootha V, Troy A, Cinti S, Lowell B, Scarpulla RC, *et al.* (1999) *Cell* 98:115–124.
14. St-Pierre J, Lin J, Krauss S, Tarr PT, Yang R, Newgard CB, Spiegelman BM (2003) *J Biol Chem* 278:26597–26603.
15. Lin J, Wu H, Tarr PT, Zhang CY, Wu Z, Boss O, Michael LF, Puigserver P, Isotani E, Olson EN, *et al.* (2002) *Nature* 418:797–801.
16. Lin J, Wu PH, Tarr PT, Lindenberg KS, St-Pierre J, Zhang CY, Mootha VK, Jager S, Vianna CR, Reznick RM, *et al.* (2004) *Cell* 119:121–135.
17. Leone TC, Lehman JJ, Finck BN, Schaeffer PJ, Wende AR, Boudina S, Courtois M, Wozniak DF, Sambandam N, Bernal-Mizrachi C, *et al.* (2005) *PLoS Biol* 3:e101.
18. Kressler D, Schreiber SN, Knutti D, Kralli A (2002) *J Biol Chem* 277:13918–13925.
19. Lin J, Puigserver P, Donovan J, Tarr P, Spiegelman BM (2002) *J Biol Chem* 277:1645–1648.
20. Meirhaeghe A, Crowley V, Lenaghan C, Lelliott C, Green K, Stewart A, Hart K, Schinner S, Sethi JK, Yeo G, *et al.* (2003) *Biochem J* 373:155–165.
21. Su AI, Wiltshire T, Batalov S, Lapp H, Ching KA, Block D, Zhang J, Soden R, Hayakawa M, Kreiman G, *et al.* (2004) *Proc Natl Acad Sci USA* 101:6062–6067.
22. Lin J, Tarr PT, Yang R, Rhee J, Puigserver P, Newgard CB, Spiegelman BM (2003) *J Biol Chem* 278:30843–30848.
23. Kamei Y, Ohizumi H, Fujitani Y, Nemoto T, Tanaka T, Takahashi N, Kawada T, Miyoshi M, Ezaki O, Kakizuka A (2003) *Proc Natl Acad Sci USA* 100:12378–12383.
24. Uldry M, Yang W, St-Pierre J, Lin J, Seale P, Spiegelman BM (2006) *Cell Metab* 3:333–341.
25. Lin J, Yang R, Tarr PT, Wu PH, Handschin C, Li S, Yang W, Pei L, Uldry M, Tontonoz P, *et al.* (2005) *Cell* 120:261–273.
26. Wolfrum C, Stoffel M (2006) *Cell Metab* 3:99–110.
27. Lowell BB, S-Susulic V, Hamann A, Lawitts JA, Himms-Hagen J, Boyer BB, Kozak LP, Flier JS (1993) *Nature* 366:740–742.
28. de Jesus LA, Carvalho SD, Ribeiro MO, Schneider M, Kim SW, Harney JW, Larsen PR, Bianco AC (2001) *J Clin Invest* 108:1379–1385.
29. Horton JD, Goldstein JL, Brown MS (2002) *J Clin Invest* 109:1125–1131.
30. Kurtz DM, Rinaldo P, Rhead WJ, Tian L, Millington DS, Vockley J, Hamm DA, Brix AE, Lindsey JR, Pinkert CA, *et al.* (1998) *Proc Natl Acad Sci USA* 95:15592–15597.
31. Vianna CR, Huntgeburth M, Coppari R, Choi CS, Lin J, Krauss S, Barbatelli G, Tzameli I, Kim YB, Cinti S, *et al.* (2006) *Cell Metab* 4:453–464.
32. Lelliott CJ, Medina-Gomez G, Petrovic N, Kis A, Feldmann HM, Bjursell M, Parker N, Curtis K, Campbell M, Hu P, *et al.* (2006) *PLoS Biol* 4:e369.
33. Golozoubova V, Hohtola E, Matthias A, Jacobsson A, Cannon B, Nedergaard J (2001) *FASEB J* 15:2048–2050.
34. Ukropec J, Anunciado RP, Ravussin Y, Hulver MW, Kozak LP (2006) *J Biol Chem* 281:31894–31908.
35. McGill JK, Beal MF (2006) *Cell* 127:465–468.
36. Villena JA, Hock MB, Chang WY, Barcas JE, Giguere V, Kralli A (2007) *Proc Natl Acad Sci USA* 104:1418–1423.